Strength predictions of pile caps by a strut-and-tie model approach

JungWoong Park, Daniel Kuchma, and Rafael Souza

Abstract: In this paper, a strut-and-tie model approach is presented for calculating the strength of reinforced concrete pile caps. The proposed method employs constitutive laws for cracked reinforced concrete and considers strain compatibility. This method is used to calculate the load-carrying capacity of 116 pile caps that have been tested to failure in structural research laboratories. This method is illustrated to provide more accurate estimates of behavior and capacity than the special provisions for slabs and footings of the 1999 American Concrete Institute (ACI) code, the pile cap provisions in the 2002 *CRSI design handbook*, and the strut-and-tie model provisions in either the 2005 ACI code or the 2004 Canadian Standards Association (CSA) A23.3 standard. The comparison shows that the proposed method consistently well predicts the strengths of pile caps with shear span-to-depth ratios ranging from 0.49 to 1.8 and concrete strengths less than 41 MPa. The proposed approach provides valuable insight into the design and behavior of pile caps.

Key words: strut-and-tie model, pile caps, footings, failure strength, shear strength.

Résumé : Cet article présente un modèle à treillis pour calculer la résistance des têtes de pieux en béton armé. La méthode proposée utilise les lois constitutives pour le béton armé fissuré et elle tient compte de la compatibilité de la déformation. Cette méthode est utilisée pour calculer la capacité portante de 116 têtes de pieux mises à l'épreuve jusqu'à défaillance dans des laboratoires de recherche structurale. Cette méthode est illustrée afin de fournir des estimations plus précises du comportement et de la capacité que celles fournies par les dispositions spéciales pour les dalles et les semelles du code 1999 de l'ACI (American Concrete Institute), les dispositions pour les têtes de pieux dans le *CRSI design handbook* de 2002 et les dispositions du modèle à treillis dans le code ACI 2005 ou dans la norme A23.3 de l'Association canadienne de normalisation (« CSA »). La comparaison montre que la méthode proposée prédit adéquatement et constamment les résistances des têtes de pieux avec des rapports de portée-épaisseur variant entre 0,49 et 1,8 et des résistances du béton inférieures à 41 MPa. L'approche proposée fournit un aperçu intéressant du comportement et de la conception des têtes de pieux.

Mots-clés : modèle à treillis, semelles, résistance à la défaillance, résistance au cisaillement.

[Traduit par la Rédaction]

Introduction

The traditional design procedure for pile caps is the same sectional approach as that typically used for the design of two-way slabs and spread footings in which the depth is selected to provide adequate shear strength from concrete alone and the required amount of longitudinal reinforcement is calculated using the engineering beam theory assumption that plane sections remain plane. However, pile caps are three-dimensional discontinuity (D) regions in which there is a complex variation in straining not adequately captured by sectional approaches. A new design procedure for all D-regions, including pile caps, has recently been introduced into North American design practice (CSA 1984; AASHTO 1994; ACI Committee 318 2002). This procedure is based on a strut-and-tie approach in which an idealized load-resisting truss is designed to carry the imposed loads through the discontinuity region to its supports. For the typically stocky pile cap, such as the four-pile cap shown in Fig. 1, this consists of compressive concrete struts that run between the column and the piles and steel reinforcement ties that extend between piles.

The strut-and-tie approach is conceptually simple and is generally regarded as an appropriate approach for the design of all D-regions. To enable its use in practice, it was necessary to develop specific rules for defining geometry and stress limits in struts and ties that have been incorporated into codes of practice. These rules and limits were principally derived from tests on planar structures and they are substantially different for the two predominant strut-and-tie design provisions in North America, those being the *Design of concrete structures* by the Canadian Standards Association (CSA) (CSA 2004) and Appendix A "strut-and-tie models" of the *Building code requirements for structural concrete* of the American Concrete Institute (ACI Committee 318 2005). An evaluation of the applicability of these strut-and-tie provisions to pile caps should be made using available experimental test data. In addition, it would be

Received 13 December 2006. Revision accepted 2 June 2008. Published on the NRC Research Press Web site at cjce.nrc.ca on 21 November 2008.

J. Park, D. Kuchma,[1] and R. Souza. Department of Civil and Environmental Engineering, University of Illinois at Urbana-Champaign, 2114 Newmark Laboratory, 205 N. Mathews Ave., Urbana, IL 61801, USA.

Written discussion of this article is welcomed and will be received by the Editor until 30 April 2009.

[1]Corresponding author (e-mail: kuchma@uiuc.edu).

 doi:10.1139/L08-062

Fig. 1. Strut-and-tie model for pile caps.

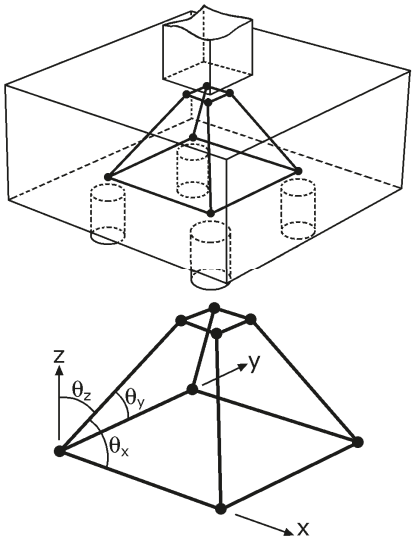

useful to assess if the design of pile caps would benefit from any additional specific rules or guidelines to ensure a safe and effective design.

This paper presents an examination of existing design methods for pile caps as well as a new strut-and-tie approach for calculating the capacity of pile caps. This new approach utilizes constitutive laws for cracked reinforced concrete and considers both strain compatibility and equilibrium. To validate the proposed method, it is also used to calculate the strength of 116 pile caps with concrete strengths less than 41 MPa. These strengths are also compared with those calculated using the special provisions for slabs and footings of ACI318–99 (ACI Committee 318 1999), the *CRSI design handbook* (CRSI 2002), the strut-and-tie model provisions used in ACI318–05 (ACI Committee 318 2005) and the CSA (2004), and the strut-and-tie model approach presented by Adebar and Zhou (1996).

Existing pile design methods

This section provides a brief discussion of the aforementioned provisions and guidelines that are used in North American practice for the design of pile caps.

ACI318–99 (ACI Committee 318 1999) and the CRSI handbook (CRSI 2002) suggest that pile caps be designed using the same sectional design approaches as those for slender footings supported on soil. This requires a design for flexure at the face of columns as well as one- and two-way shear checks. The CRSI handbook provides an additional relationship for evaluating V_c when the shear span is less than one-half the depth of the member, $w < d/2$, as presented in eq. [1] where c is the dimension of a square column. These procedures are the most commonly used in North American design practice.

$$[1] \qquad V_c = \left(\frac{d}{w}\right)\left(1+\frac{d}{c}\right)(0.33\sqrt{f'_c})\ b_s d$$

where f'_c has a unit of MPa and the shear section perimeter is $b_s = 4c$. A more complete definition of symbols is presented in the "List of symbols" at the end of this paper.

Appendix A of ACI318–05 (ACI Committee 318 2005) and CSA A23.3 CSA (2004) provide provisions for the design of all D-regions in structural concrete, including pile caps. These provisions include dimensioning rules as well as stress limits for evaluating the capacity of struts, nodes, and the anchorage region of ties. They principally differ in the stress limits for struts. In ACI318–05, the compressive stress for the type of bottle-shaped struts that occur in pile caps would be $0.51f'_c$. The stress limit in struts by the CSA A23.3 strut-and-tie provisions are a function of the angle of the strut relative to the longitudinal axis, with the effect that the stress limit in 30°, 45°, and 60° struts with the assumption of tie strain $\varepsilon_s = 0.002$ would be $0.31f'_c$, $0.55f'_c$, and $0.73f'_c$, respectively. The strut-and-tie provisions in these code and standard specifications have only had limited use in design practice.

Based on an analytical and experimental study of compression struts confined by plain concrete, Adebar and Zhou (1993) concluded that the design of pile caps should include a check on bearing strength that is a function of the amount of confinement and the aspect ratio of the diagonal struts. Adebar and Zhou (1996) provided the following equations for the maximum allowable bearing stress in nodal zones:

$$[2] \qquad f_b \le 0.6f'_c + 6\alpha\beta\sqrt{f'_c}$$

$$[3] \qquad \alpha = \frac{1}{3}(\sqrt{A_2/A_1} - 1) \le 1.0$$

$$[4] \qquad \beta = \frac{1}{3}\left(\frac{h_s}{b_s} - 1\right) \le 1.0$$

The parameters α and β account for the confinement of the compression strut and the geometry of the diagonal strut. The ratio A_2/A_1 in eq. [3] is identical to that used in ACI318–05 for calculating the bearing strength. The ratio h_s/b_s is the aspect ratio (height to width) of the strut. Adebar and Zhou (1996) suggested that the check described above be added to the traditional section force approach for pile cap design.

The calculated strengths by these provisions and design guidelines are compared against a test database following the presentation of the authors' proposed strut-and-tie method and this test database. As presented later, the accuracy of the current code and standard methods for pile cap design is not satisfactory and is uncertain for members beyond the dataset from which they were derived. It is, therefore, desirable to have an improved design philosophy that is based on a complete resistance model and is calibrated to provide improved accuracy for the range of available test data.

Three-dimensional strut-and-tie model approach

To further evaluate the effectiveness of a strut-and-tie design approach for pile caps and to identify means of improving design provisions, a methodology for evaluating the capacity of pile caps was developed that considers strain compatibility and uses a nonlinear constitutive relationship for evaluating the strength of struts. The authors focused

Table 1. Test data of Clarke (1973).

Pile cap	f'_c (MPa)	Cap size (mm × mm)	l_e (mm)	(a)	Bar arrangement
A1	21.3	950×950	600	10	Grid
A2	27.2	950×950	600	10	Bunched
A4	21.4	950×950	600	10	Grid
A5	26.6	950×950	600	10	Bbunched
A7	24.2	950×950	600	10	Grid
A8	27.2	950×950	600	10	Bunched
A9	26.6	950×950	600	10	Grid
A10	18.8	950×950	600	10	Grid
A11	18.0	950×950	600	10	Grid
A12	25.3	950×950	600	10	Grid
B1	26.7	750×750	400	8	Grid
B2	24.5	750×750	400	10	Grid
B3	35.0	750×750	400	6	Grid

Note: (a), number of D10 bars at both x and y directions; yield strength of reinforcement f_y = 410 MPa, overall height h = 450 mm, effective depth d = 405 mm, column width c = 200 mm, and pile diameter d_p = 200 mm for all specimens.

their study on four-pile caps as the majority of test data and a substantial portion of in-field applications are for this type of structure. Extension to other configurations is feasible providing that reasonable estimates can be made for pile forces distributions in caps supported by larger numbers of piles. In this procedure, the three-dimensional strut-and-tie model shown in Fig. 1 was used for the idealized load-resisting truss in a four-pile cap. This model is used for all pile caps examined in this paper. The shear span-to-depth ratio of most test specimens selected in this study is less than one. As the mode of failure is not known for all test specimens, the proposed model considers the possibility of crushing of the compression zone at the base of the column and yielding of the longitudinal reinforcement (ties). For all truss models used in this study, the angle between longitudinal ties and diagonal struts is greater than 25°, satisfying the ACI318–05 (ACI Committee 318 2005) limit. The details of the proposed strut-and-tie approach are now presented.

Effective depth of concrete strut

The effective strut width is assumed to be based on the available concrete area and the anchorage conditions of the strut. The effective area of the diagonal strut at the top node is taken as

$$[5] \qquad A_d = \frac{c}{\sqrt{2}}\left(\frac{c}{\sqrt{2}}\cos\theta_z + kd\sin\theta_z\right)$$

where k is derived from the bending theory for a single reinforced section as follows:

$$[6] \qquad k = \sqrt{(n\rho)^2 + 2n\rho} - n\rho$$

and where n is the ratio of steel to concrete elastic moduli with E_c taken as follows (Martinez et al. 1982)

$$[7] \qquad E_c = \begin{cases} 4730\sqrt{f'_c} & \text{for } f'_c \le 21 \text{ MPa} \\ 3320\sqrt{f'_c} + 6900 & \text{for } f'_c > 21 \text{ MPa} \end{cases}$$

The inclination angles between the diagonal struts and the x-, y-, and z-axis are expressed as θ_x, θ_y, and θ_z, respectively, as shown in Fig. 1. These angles represent the direction cosines of a diagonal strut. The effective area of a diagonal strut at the bottom node is taken as

$$[8] \qquad A_d = \frac{\pi}{4} d_p[d_p\cos\theta_z + 2(h-d)\sin\theta_z]$$

where d_p is pile diameter and h is overall height of the pile cap. The effective area of the diagonal strut is taken as the smaller of eqs. [5] and [8]. The pile axial load capacity can be examined using the nonlinear load transfer curves (Kim et al. 2007), but it is beyond the scope of this study.

The effective depth of a horizontal strut is taken as $h/4$ for pile caps based on the suggestion of Paulay and Priestley (1992) on the depth of the flexural compression zone of the elastic column as follows:

$$[9] \qquad w_c = \left(0.25 + 0.85\frac{N}{A_g f'_c}\right) h_c$$

where N is the compression force acting on the column, A_g is the gross area of the column section, and h_c is the overall height of the column section.

Force equilibrium

The strut-and-tie model shown in Fig. 1 is statically determinate and thus, member forces can be calculated from the equilibrium equations only as given below:

$$[10] \qquad F_d = \frac{P}{4\cos\theta_y}$$

$$[11] \qquad F_x = F_d\cos\theta_x$$

$$[12] \qquad F_y = F_d\cos\theta_y$$

where P is the column load; F_d is the compressive forces in the diagonal strut; F_x and F_y are, respectively, the member forces in the x- and y-axis horizontal struts and ties. As the

Table 2. Test data of Suzuki et al. (1998).

Pile cap	f'_c (MPa)	Cap size (mm × mm)	l_e (mm)	h (mm)	d (mm)	c (mm)	(a)	f_y (MPa)		Bar arrangement
								x dir.	y dir.	
								413	413	Grid
BP-20–2	20.4	900×900	540	200	150	300	8	413	413	Grid
BPC-20–1	21.9	900×900	540	200	150	300	8	413	413	Bunched
BPC-20–2	19.9	900×900	540	200	150	300	8	413	413	Bunched
BP-25–1	22.6	900×900	540	250	200	300	10	413	413	Grid
BP-25–2	21.5	900×900	540	250	200	300	10	413	413	Grid
BPC-25–1	18.9	900×900	540	250	200	300	10	413	413	Bunched
BPC-25–2	22.0	900×900	540	250	200	300	10	413	413	Bunched
BP-20–30–1	29.1	800×800	500	200	150	300	6	405	405	Grid
BP-20–30–2	29.8	800×800	500	200	150	300	6	405	405	Grid
BPC-20–30–1	29.8	800×800	500	200	150	300	6	405	405	Bunched
BPC-20–30–2	29.8	800×800	500	200	150	300	6	405	405	Bunched
BP-30–30–1	27.3	800×800	500	300	250	300	8	405	405	Grid
BP-30–30–2	28.5	800×800	500	300	250	300	8	405	405	Grid
BPC-30–30–1	28.9	800×800	500	300	250	300	8	405	405	Bunched
BPC-30–30–2	30.9	800×800	500	300	250	300	8	405	405	Bunched
BP-30–25–1	30.9	800×800	500	300	250	250	8	405	405	Grid
BP-30–25–2	26.3	800×800	500	300	250	250	8	405	405	Grid
BPC-30–25–1	29.1	800×800	500	300	250	250	8	405	405	Bunched
BPC-30–25–2	29.2	800×800	500	300	250	250	8	405	405	Bunched
BDA-70–90–1	29.1	700×900	500	300	250	250	8	356	345	Grid
BDA-70–90–2	30.2	700×900	500	300	250	250	8	356	345	Grid
BDA-80–90–1	29.1	800×900	500	300	250	250	8	356	345	Grid
BDA-80–90–2	29.3	800×900	500	300	250	250	8	356	345	Grid
BDA-90–90–1	29.5	900×900	500	300	250	250	8	356	345	Grid
BDA-90–90–2	31.5	900×900	500	300	250	250	8	356	345	Grid
BDA-100–90–1	29.7	1000×900	500	300	250	250	8	356	345	Grid
BDA-100–90–2	31.3	1000×900	500	300	250	250	8	356	345	Grid

Note: (a), number of D10 bars at both of x (x dir.) and y (y dir.) directions; pile diameter d_p = 150 mm for all specimens.

strut-and-tie method is a full member design procedure; flexure and shear are not explicitly considered.

Constitutive laws

Cracked reinforced concrete can be treated as an orthotropic material with its principal axes corresponding to the directions of the principal average tensile and compressive strains. Cracked concrete subjected to high tensile strains in the direction normal to the compression is observed to be softer than concrete in a standard cylinder test (Hsu and Zhang 1997; Vecchio and Collins 1982, 1986, 1993). This phenomenon of strength and stiffness reduction is commonly referred to as compression softening. Applying this softening effect to the strut-and-tie model, it is recognized that the tensile straining perpendicular to the compression strut will reduce the capacity of the concrete strut to resist compressive stresses. Multiple compression softening models were used in this study to investigate the sensitivity of the results to the selected model. All models were found to provide similarly good results as will be illustrated later in the paper. The compression-softening model proposed by Hsu and Zhang (1997) was selected for the base comparisons and is now described, but it has been illustrated by the authors in an earlier paper (Park and Kuchma 2007) that different compression-softening models can be similarly used. The stress of the concrete strut is determined from the following equations proposed by Hsu and Zhang (1997):

$$[13] \qquad \sigma_d = \xi f'_c \left[2\left(\frac{\varepsilon_d}{\xi\varepsilon_0}\right) - \left(\frac{\varepsilon_d}{\xi\varepsilon_0}\right)^2 \right] \qquad \text{for } \frac{\varepsilon_d}{\xi\varepsilon_0} \le 1$$

$$[14] \qquad \sigma_d = \xi f'_c \left\{ 1 - \left[\frac{\varepsilon_d/(\xi\varepsilon_0) - 1}{2/\xi - 1} \right]^2 \right\} \qquad \text{for } \frac{\varepsilon_d}{\xi\varepsilon_0} > 1$$

$$[15] \qquad \xi = \frac{5.8}{\sqrt{f'_c}} \frac{1}{\sqrt{1 + 400\varepsilon_r}} \le \frac{0.9}{\sqrt{1 + 400\varepsilon_r}}$$

where ε_d is a compressive strain of the concrete strut, ξ is a concrete-softening coefficient, ε_r is a tensile strain of the direction perpendicular to the concrete strut, ε_0 is a concrete cylinder strain corresponding to the cylinder strength f'_c, which can be defined approximately as (Foster and Gilbert 1996)

$$[16] \qquad \varepsilon_0 = 0.002 + 0.001 \left(\frac{f'_c - 20}{80} \right) \qquad \text{for } 20 \le f'_c \le 100 \text{ MPa}$$

Table 3. Test data of Suzuki et al. (1999).

Pile cap	f'_c (MPa)	l_e (mm)	h (mm)	d (mm)	(a)	(b)
TDL1–1	30.9	600	350	300	4	356
TDL1–2	28.2	600	350	300	4	356
TDL2–1	28.6	600	350	300	6	356
TDL2–2	28.8	600	350	300	6	356
TDL3–1	29.6	600	350	300	8	356
TDL3–2	29.3	600	350	300	8	356
TDS1–1	25.6	450	350	300	6	356
TDS1–2	27.0	450	350	300	6	356
TDS2–1	27.2	450	350	300	8	356
TDS2–2	27.3	450	350	300	8	356
TDS3–1	28.0	450	350	300	11	356
TDS3–2	28.1	450	350	300	11	356
TDM1–1	27.5	500	300	250	4	383
TDM1–2	26.3	500	300	250	4	383
TDM2–1	29.6	500	300	250	6	383
TDM2–2	27.6	500	300	250	6	383
TDM3–1	27.0	500	300	250	10	370
TDM3–2	28.0	500	300	250	10	370

Note: (a), number of D10 bars at both of x and y directions; (b), yield strength of reinforcement at both of x and y directions in MPa; pile cap size 900 × 900 mm, column width c = 250 mm, pile diameter d_p = 150 mm, grid type of bar arrangement for all specimens.

The response of the ties is based on the linear elastic perfectly plastic assumption.

$$[17] \qquad F_{st} = E_s A_{st} \varepsilon_{st} \leq F_{st}$$

where A_{st} and F_{st} are, respectively, the area and yielding force of a horizontal steel tie in the x- or y-axis.

The proposed method considers a tension stiffening effect for evaluating the force and strain in steel ties. Vecchio and Collins (1986) suggested the following relationship for evaluating the average tensile stress in cracked concrete:

$$[18] \qquad f_{ct} = \frac{f_{cr}}{1 + \sqrt{200\varepsilon_r}}$$

Taking f_{cr} as $0.33\sqrt{f'_c}$ and ε_r as 0.002, the tension force resisted by the concrete tie is given by

$$[19] \qquad F_{ct} = 0.20\sqrt{f'_c} A_{ct}$$

where A_{ct} is the effective area of concrete tie, which is taken as

$$[20] \qquad A_{ct} = \frac{d}{4}\left(\frac{l_e}{2} + \frac{d_p}{2}\right)$$

where l_e is the pile spacing.

Compatibility relations

The strain compatibility relation used in this study is the sum of normal strain in two perpendicular directions, which is an invariant as the sum of the strains is constant

$$[21] \qquad \varepsilon_h + \varepsilon_v = \varepsilon_r + \varepsilon_d$$

Equation [21] can be obtained from strain compatibility as represented using the Mohr's circle of strain. As horizontal and vertical web reinforcements were not available from test data, ε_h and ε_v are conservatively taken as 0.002 in eq. [21].

Procedure for evaluating the capacity of pile caps

The procedure for calculating the capacity of piles caps by the authors' proposed method uses the compatibility, equilibrium, and constitutive relationships as described above and is as follows:

(1) According to the member forces calculated from eq. [10] to eq. [12], ε_d and ε_r are found for P using eq. [13] and eq. [21], respectively. A concrete-softening coefficient ξ is calculated from eq. [15] using ε_r.

(2) The updated value of σ_d is calculated from eq. [13]. If the difference between the two σ_d values is larger than the defined tolerance, the steps are repeated until convergence has been achieved. Nominal strength by failure of the diagonal strut can be estimated from

$$[22] \qquad P_n = 4\xi f'_c A_d \cos\theta_z$$

(3) The nominal strength by failure of horizontal concrete strut is taken as

$$[23] \qquad P_n = 0.85 f'_c \frac{hc}{2}\frac{\cos\theta_z}{\cos\theta_x}$$

and the nominal strength by tension failure mode can be expressed as

$$[24] \qquad P_n = (2 f_y A_s + 4F_{ct})\frac{\cos\theta_z}{\cos\theta_x}$$

where f_y and A_s are the yield strength and cross-sectional area of the bottom longitudinal reinforcement, respectively. The strength of the pile cap by a tension failure

Table 4. Test data of Suzuki et al. (2000).

Pile cap	f'_c (MPa)	Cap size (mm × mm)	h (mm)	d (mm)	c (mm)	(a)	(b)
BDA-20–25–70–1	26.1	700×700	200	150	250	4	358
BDA-20–25–70–2	26.1	700×700	200	150	250	4	358
BDA-20–25–80–1	25.4	800×800	200	150	250	4	358
BDA-20–25–80–2	25.4	800×800	200	150	250	4	358
BDA-20–25–90–1	25.8	900×900	200	150	250	4	358
BDA-20–25–90–2	25.8	900×900	200	150	250	4	358
BDA-30–20–70–1	25.2	700×700	300	250	200	6	358
BDA-30–20–70–2	24.6	700×700	300	250	200	6	358
BDA-30–20–80–1	25.2	800×800	300	250	200	6	358
BDA-30–20–80–2	26.6	800×800	300	250	200	6	358
BDA-30–20–90–1	26.0	900×900	300	250	200	6	358
BDA-30–20–90–2	26.1	900×900	300	250	200	6	358
BDA-30–25–70–1	28.8	700×700	300	250	250	6	383
BDA-30–25–70–2	26.5	700×700	300	250	250	6	383
BDA-30–25–80–1	29.4	800×800	300	250	250	6	383
BDA-30–25–80–2	27.8	800×800	300	250	250	6	383
BDA-30–25–90–1	29.0	900×900	300	250	250	6	383
BDA-30–25–90–2	26.8	900×900	300	250	250	6	383
BDA-30–30–70–1	26.8	700×700	300	250	300	6	358
BDA-30–30–70–2	25.9	700×700	300	250	300	6	358
BDA-30–30–80–1	27.4	800×800	300	250	300	6	358
BDA-30–30–80–2	27.4	800×800	300	250	300	6	358
BDA-30–30–90–1	27.2	900×900	300	250	300	6	358
BDA-30–30–90–2	24.5	900×900	300	250	300	6	358
BDA-40–25–70–1	25.9	700×700	400	350	250	8	358
BDA-40–25–70–2	24.8	700×700	400	350	250	8	358
BDA-40–25–80–1	26.5	800×800	400	350	250	8	358
BDA-40–25–80–2	25.5	800×800	400	350	250	8	358
BDA-40–25–90–1	25.7	900×900	400	350	250	8	358
BDA-40–25–90–2	26.0	900×900	400	350	250	8	358

Note: (a), number of D10 bars at both of x and y directions; (b), yield strength of reinforcement at both of x and y directions in MPa; pile spacing l_e = 450 mm, pile diameter d_p = 150 mm, and grid type of bar arrangement for all specimens.

Table 5. Test data of Suzuki and Otsuki (2002).

Pile cap	f'_c (MPa)	c (mm)	Anchorage
BPL-35–30–1	24.1	300	180° hook
BPL-35–30–2	25.6	300	180° hook
BPB-35–30–1	23.7	300	Bent up
BPB-35–30–2	23.5	300	Bent up
BPH-35–30–1	31.5	300	180° hook
BPH-35–30–2	32.7	300	180° hook
BPL-35–25–1	27.1	250	180° hook
BPL-35–25–2	25.6	250	180° hook
BPB-35–25–1	23.2	250	Bent up
BPB-35–25–2	23.7	250	Bent up
BPH-35–25–1	36.6	250	180° hook
BPH-35–25–2	37.9	250	180° hook
BPL-35–20–1	22.5	200	180° hook
BPL-35–20–2	21.5	200	180° hook
BPB-35–20–1	20.4	200	Bent up
BPB-35–20–2	20.2	200	Bent up
BPH-35–20–1	31.4	200	180° hook
BPH-35–20–2	30.8	200	180° hook

Note: Nine D10 bars at both of x and y directions; yield strength of reinforcement f_y = 353 MPa, pile cap size 800 mm × 800 mm, pile spacing l_e = 500 mm, overall height h = 350 mm, effective depth d = 300 mm, pile diameter d_p = 150 mm, and grid type of bar arrangement for all specimens.

Table 6. Test data of Sabnis and Gogate (1984).

Pile cap	f'_c (MPa)	d (mm)	(a)	(b)
SS1	31.3	111	0.0021	499
SS2	31.3	112	0.0014	662
SS3	31.3	111	0.00177	886
SS4	31.3	112	0.0026	482
SS5	41.0	109	0.0054	498
SS6	41.0	109	0.0079	499
SG1	17.9	152	0	—
SG2	17.9	117	0.0055	414
SG3	17.9	117	0.0133	414

Note: (a), reinforcement ratio at both of x and y directions; (b), yield strength of reinforcement at both of x and y directions in MPa; pile cap size 330 mm × 330 mm, pile spacing l_e = 203 mm, overall height h = 152 mm, column diameter c = 76 mm, pile diameter d_p = 76 mm, and grid type of bar arrangement for all specimens.

mode is the column load to cause yielding of the reinforcement and fracture of a concrete tie.

(4) The predicted strength by this method is the minimum value of the nominal strengths computed from the different failure modes, which are crushing or splitting of the diagonal concrete strut, crushing of the compression zone at the base of the column load, and yielding of longitudinal reinforcement.

Table 7. Ratio of measured to predicted strength.

		P_{test}/P_n					
Specimen	P_{test} (kN)	(a)	(b)	(c)	(d)	(e)	(f)
		2.08	2.08	1.69	1.8	1.43	1.51
BP-20–2	480	1.93	1.93	1.57	1.67	1.32	1.45
BPC-20–1	519	2.08	2.08	1.69	1.8	1.43	1.48
BPC-20–2	529	2.13	2.13	1.73	1.84	1.46	1.64
BP-25–1	735	1.76	1.76	1.52	1.46	1.22	1.51
BP-25–2	755	1.81	1.81	1.64	1.51	1.25	1.63
BPC-25–1	818	1.98	1.98	2.02	1.64	1.35	2.01
BPC-25–2	813	1.95	1.95	1.73	1.62	1.35	1.72
BP-20–30–1	485	2.40	2.40	1.93	2.02	1.63	1.62
BP-20–30–2	480	2.38	2.38	1.91	2.00	1.62	1.60
BPC-20–30–1	500	2.48	2.48	1.99	2.08	1.68	1.67
BPC-20–30–2	495	2.45	2.45	1.97	2.06	1.67	1.65
BP-30–30–1	916	2.03	2.03	1.52	1.58	1.39	1.34
BP-30–30–2	907	2.01	2.01	1.5	1.57	1.37	1.32
BPC-30–30–1	1039	2.30	2.3	1.72	1.79	1.57	1.51
BPC-30–30–2	1029	2.28	2.28	1.71	1.77	1.56	1.49
BP-30–25–1	794	1.76	1.76	1.44	1.51	1.29	1.23
BP-30–25–2	725	1.61	1.61	1.32	1.39	1.18	1.14
BPC-30–25–1	853	1.89	1.89	1.55	1.62	1.38	1.33
BPC-30–25–2	872	1.93	1.93	1.58	1.66	1.42	1.36
BDA-70–90–1	784	1.97	1.97	1.62	1.70	1.45	1.36
BDA-70–90–2	755	1.89	1.89	1.56	1.63	1.39	1.30
BDA-80–90–1	858	2.15	2.15	1.77	1.86	1.58	1.49
BDA-80–90–2	853	2.14	2.14	1.76	1.85	1.58	1.48
BDA-90–90–1	853	2.14	2.14	1.76	1.84	1.58	1.48
BDA-90–90–2	921	2.31	2.31	1.9	1.99	1.7	1.59
BDA-100–90–1	911	2.28	2.28	1.88	1.97	1.68	1.58
BDA-100–90–2	931	2.33	2.33	1.92	2.01	1.72	1.60
A1	1110	1.44	1.44	1.73	1.53	1.17	1.10
A2	1420	1.83	1.83	1.73	1.74	1.50	1.33
A4	1230	1.59	1.59	1.91	1.69	1.30	1.22
A5	1400	1.80	1.8	1.75	1.72	1.48	1.31
A7	1640	2.12	2.12	2.25	2.03	1.73	1.55
A8	1510	1.95	1.95	1.84	1.85	1.59	1.41
A9	1450	1.87	1.87	1.81	1.78	1.53	1.36
A10	1520	1.97	1.97	2.68	2.38	1.60	1.71
A11	1640	2.13	2.13	3.02	2.68	1.73	1.92
A12	1640	2.12	2.12	2.15	2.02	1.73	1.55
B1	2080	2.23	2.23	2.29	2.29	1.65	1.79
B2	1900	1.64	1.64	2.28	2.28	1.20	1.78
B3	1770	2.52	2.52	1.97	2.06	1.87	1.50
BPL-35–30–1	960	1.81	1.81	1.32	1.38	1.24	1.26
BPL-35–30–2	941	1.77	1.77	1.3	1.35	1.21	1.18
BPB-35–30–1	1029	1.94	1.94	1.42	1.48	1.32	1.38
BPB-35–30–2	1103	2.08	2.08	1.52	1.59	1.42	1.49
BPH-35–30–1	980	1.83	1.83	1.35	1.40	1.26	1.16
BPH-35–30–2	1088	2.04	2.04	1.5	1.55	1.40	1.28
BPL-35–25–1	902	1.69	1.69	1.36	1.42	1.24	1.16
BPL-35–25–2	872	1.64	1.64	1.31	1.38	1.20	1.13
BPB-35–25–1	911	1.72	1.72	1.37	1.45	1.26	1.30
BPB-35–25–2	921	1.73	1.73	1.38	1.46	1.27	1.29
BPH-35–25–1	882	1.65	1.65	1.33	1.38	1.22	1.10
BPH-35–25–2	951	1.78	1.78	1.43	1.49	1.31	1.18
BPL-35–20–1	755	1.42	1.42	1.24	1.33	1.11	1.15
BPL-35–20–2	735	1.39	1.39	1.21	1.30	1.08	1.17
BPB-35–20–1	755	1.43	1.43	1.31	1.34	1.11	1.27

Table 7 (*continued*).

		P_{test}/P_n					
Specimen	P_{test} (kN)	(a)	(b)	(c)	(d)	(e)	(f)
BPB-35–20–2	804	1.52	1.52	1.41	1.43	1.18	1.37
BPH-35–20–1	813	1.52	1.52	1.33	1.41	1.20	1.10
BPH-35–20–2	794	1.49	1.49	1.30	1.38	1.17	1.08
BDA-20–25–70–1	294	2.22	2.22	1.93	2.03	1.57	1.46
BDA-20–25–70–2	304	2.29	2.29	1.99	2.10	1.62	1.51
BDA-20–25–80–1	304	2.29	2.29	1.99	2.10	1.62	1.51
BDA-20–25–80–2	304	2.29	2.29	1.99	2.10	1.62	1.51
BDA-20–25–90–1	333	2.50	2.50	2.18	2.30	1.77	1.65
BDA-20–25–90–2	333	2.50	2.50	2.18	2.30	1.77	1.65
BDA-30–20–70–1	534	1.61	1.61	1.40	1.50	1.23	1.12
BDA-30–20–70–2	549	1.65	1.65	1.44	1.54	1.26	1.16
BDA-30–20–80–1	568	1.71	1.71	1.49	1.60	1.30	1.19
BDA-30–20–80–2	564	1.69	1.69	1.48	1.58	1.29	1.18
BDA-30–20–90–1	583	1.75	1.75	1.53	1.64	1.34	1.22
BDA-30–20–90–2	588	1.76	1.76	1.54	1.65	1.35	1.23
BDA-30–25–70–1	662	1.86	1.86	1.47	1.54	1.32	1.21
BDA-30–25–70–2	676	1.90	1.90	1.50	1.57	1.35	1.24
BDA-30–25–80–1	696	1.95	1.95	1.54	1.62	1.39	1.27
BDA-30–25–80–2	725	2.03	2.03	1.61	1.69	1.44	1.33
BDA-30–25–90–1	764	2.14	2.14	1.69	1.78	1.52	1.39
BDA-30–25–90–2	764	2.14	2.14	1.69	1.78	1.52	1.40
BDA-30–30–70–1	769	2.31	2.31	1.64	1.72	1.51	1.38
BDA-30–30–70–2	730	2.20	2.20	1.56	1.63	1.44	1.31
BDA-30–30–80–1	828	2.48	2.48	1.77	1.85	1.63	1.48
BDA-30–30–80–2	809	2.43	2.43	1.73	1.81	1.59	1.44
BDA-30–30–90–1	843	2.52	2.52	1.8	1.88	1.66	1.51
BDA-30–30–90–2	813	2.44	2.44	1.74	1.81	1.60	1.47
BDA-40–25–70–1	1019	1.64	1.64	1.24	1.29	1.16	1.12
BDA-40–25–70–2	1068	1.72	1.72	1.3	1.35	1.22	1.23
BDA-40–25–80–1	1117	1.79	1.79	1.36	1.41	1.28	1.20
BDA-40–25–80–2	1117	1.80	1.80	1.36	1.41	1.28	1.25
BDA-40–25–90–1	1176	1.89	1.89	1.43	1.49	1.34	1.31
BDA-40–25–90–2	1181	1.89	1.89	1.43	1.49	1.35	1.30
TDL1–1	392	1.94	1.94	1.68	1.74	1.53	1.06
TDL1–2	392	1.95	1.95	1.68	1.74	1.53	1.08
TDL2–1	519	1.72	1.72	1.48	1.54	1.35	1.10
TDL2–2	472	1.57	1.57	1.35	1.40	1.23	1.00
TDL3–1	608	1.52	1.52	1.30	1.35	1.19	1.04
TDL3–2	627	1.57	1.57	1.34	1.39	1.22	1.07
TDS1–1	921	2.30	2.30	1.77	1.85	1.64	1.44
TDS1–2	833	2.08	2.08	1.60	1.67	1.48	1.29
TDS2–1	1005	1.89	1.89	1.45	1.52	1.34	1.24
TDS2–2	1054	1.98	1.98	1.52	1.59	1.41	1.30
TDS3–1	1299	1.78	1.78	1.40	1.44	1.26	1.42
TDS3–2	1303	1.79	1.79	1.40	1.45	1.26	1.42
TDM1–1	490	2.27	2.27	1.88	1.97	1.68	1.37
TDM1–2	461	2.13	2.13	1.77	1.85	1.58	1.30
TDM2–1	657	2.03	2.03	1.68	1.76	1.50	1.35
TDM2–2	657	2.04	2.04	1.68	1.76	1.50	1.36
TDM3–1	1245	1.53	1.44	1.72	1.21	0.99	1.72
TDM3–2	1210	1.46	1.38	1.61	1.17	0.97	1.63
SS1	250	3.04	3.04	2.76	2.96	2.48	2.31
SS2	245	3.40	3.40	3.07	3.23	2.78	2.52
SS3	248	2.04	2.04	2.71	2.04	1.65	1.72
SS4	226	2.32	2.32	2.42	2.29	1.89	1.81
SS5	264	1.61	1.61	2.21	1.66	1.09	1.43

Table 7 (*concluded*).

		P_{test}/P_n					
Specimen	P_{test} (kN)	(a)	(b)	(c)	(d)	(e)	(f)
SS6	280	1.71	1.71	2.34	1.76	1.16	1.52
SG1	50	—	—	—	—	—	1.53
SG2	173	1.43	1.43	3.11	2.49	1.2	1.97
SG3	177	1.46	1.46	3.2	2.55	1.23	2.01
Average	—	**1.97**	**1.96**	**1.73**	**1.74**	**1.44**	**1.41**
Coefficient of variation	—	**0.17**	**0.17**	**0.24**	**0.2**	**0.18**	**0.18**

Note: (a), Special provisions for slabs and footings of ACI318–99 (ACI Committtee 318 1999); (b), *CRSI design handbook* 2002 (CRSI 2002); (c), strut-and-tie model of ACI318–05 (ACI Committtee 318 2005); (d), strut-and-tie model of CSA A23.3 (CSA 2004); (e), strut-and-tie model approach of Adebar and Zhou (1996); (f), proposed strut-and-tie model approach.

Comparison with test results

Existing test data

Blévot and Frémy (1967) tested 59 four-pile caps. The majority of the four-pile caps were approximately half-scale specimens, and eight of them were full-scale with 750–1000 mm overall heights. As one of main objectives of this work was to verify a truss analogy method, they used different reinforcement details including no main reinforcement and either uniformly distributed or bunched reinforcement between piles. Clarke (1973) tested 15 square four-pile caps with overall heights of 450 mm, all approximately half-scale. Two specimens had diagonal main reinforcement, three had main reinforcement bunched over the piles, and the remaining 10 had uniformly distributed main reinforcement. The main variables in this study were pile spacing, reinforcement layout, and anchorage type. He reported that the first cracks formed on the centerlines of the vertical faces, these cracks progressed rapidly upwards forming a cruciform pattern, and finally, each cap split into four blocks. Such observations point strongly to a bending failure mode developing. However, though Clarke contended that the majority of the caps failed in shear, the authors agree with Bloodworth et al. (2003) that many of these failure modes may be more accurately described as combined bending and shear failure. Sabnis and Gogate (1984) tested nine small-scale four-pile caps with 152 mm overall heights, of which one was unreinforced. They studied how the quantity of uniformly distributed longitudinal reinforcement influences the shear capacity of deep pile caps. They reported that cracking of the four outer faces was about the same in all the specimens and is indicative of combinations of deep beam failure with very steep shear cracks and punching shear failures of slabs. They also observed that some of this cracking may be prevented by the use of horizontal reinforcement on the vertical faces of the caps; this reinforcement is only of secondary benefit and may not substantially enhance the strength of the pile cap. Adebar et al. (1990) tested six full-scale pile caps to study the performance of the strut-and-model methodology for pile cap design. Four of their tests were on diamond-shaped caps, one was on a cruciform-shaped cap, and one was on a rectangular six-pile cap. The test results demonstrated that the strain distributions are highly nonlinear both prior to and after cracking. They reported that the failure occured after a compression strut split longitudinally due to the transverse tension caused by spreading of the compressive stresses and that the maximum bearing stress is a good indicator of the likelihood of a strut splitting failure. From the pile caps they tested, the maximum bearing stress at failure had a lower limit of about $1.1f'_c$. They concluded that the strut-and-tie models accurately represent the behavior of deep pile caps and correctly suggest that the load at which a lightly reinforced pile cap fails in two-way shear depends on the quantity of longitudinal reinforcement. Suzuki et al. (1998, 1999, 2000) and Suzuki and Otsuki (2002) tested 94 four-pile caps with the reinforcement bunched over the piles or distributed in a uniform grid. The main variables investigated in these tests were the influence of edge distance, bar arrangement, taper, and concrete strength on the failure mode and the ultimate strength. They reported that it was experimentally observed that the ultimate strength of the pile caps with a uniform grid arrangement was lower than that of pile caps with an equivalent amount of reinforcement concentrated (bunched) between the pile bearings.

Though pile caps may be designed to any shape depending on the pile arrangement, only rectangular four-pile caps that had been previously tested were chosen for examination in this study. Therefore, the 116 pile cap specimens tested by Clarke (1973), Suzuki et al. (1998, 1999, 2000), Suzuki and Otsuki (2002), and Sabnis and Gogate (1984) were selected to validate the proposed method. The details of the test specimens are presented for each of the six groups of test results in Tables 1–6.

Strength prediction

The calculated strengths by the six previously discussed methods [special provisions for slabs and footings of ACI318–99 (ACI Committee 318 1999) and in the *CRSI design handbook* (CRSI 2002), and the strut-and-tie methods in ACI318–05 (ACI Committee 318 2005), CSA A23.3 (CSA 2004), by Adebar and Zhou (1996), and by the authors] are compared with the measured capacity of the 116 selected pile caps test results. In all cases, the resistance factors were set to 1.0. The details of the test specimens and strength ratios (P_{test}/P_n) are presented for each of the six groups of test results in Tables 1, 2, 3, 4, 5, 6, and collectively in Table 7 and Figs. 2–3. In all figures, the shear span a is defined by the distance from the pile centerline to the column centerline measured parallel to pile cap side. Table 8 shows the specimens that were reported to have failed by shear. The height of the specimens of Sabnis and Gogate (1984) is 152 mm, which is about a half of the code (ACI

Fig. 2. Ratio of measured-to-predicted strength with respect to shear span-to-depth ratio: (*a*) special provisions for slabs and footings of ACI318–99 (ACI Committee 318 1999); (*b*) *CRSI design handbook* 2002 (CRSI 2002); (*c*) strut-and-tie model of ACI318–05 (ACI Committee 318 2005); (*d*) strut-and-tie model of CSA A23.3 (CSA 2004); (*e*) strut-and-tie model approach of Adebar and Zhou (1996); (*f*) proposed strut-and-tie model approach. COV, coefficient of variation.

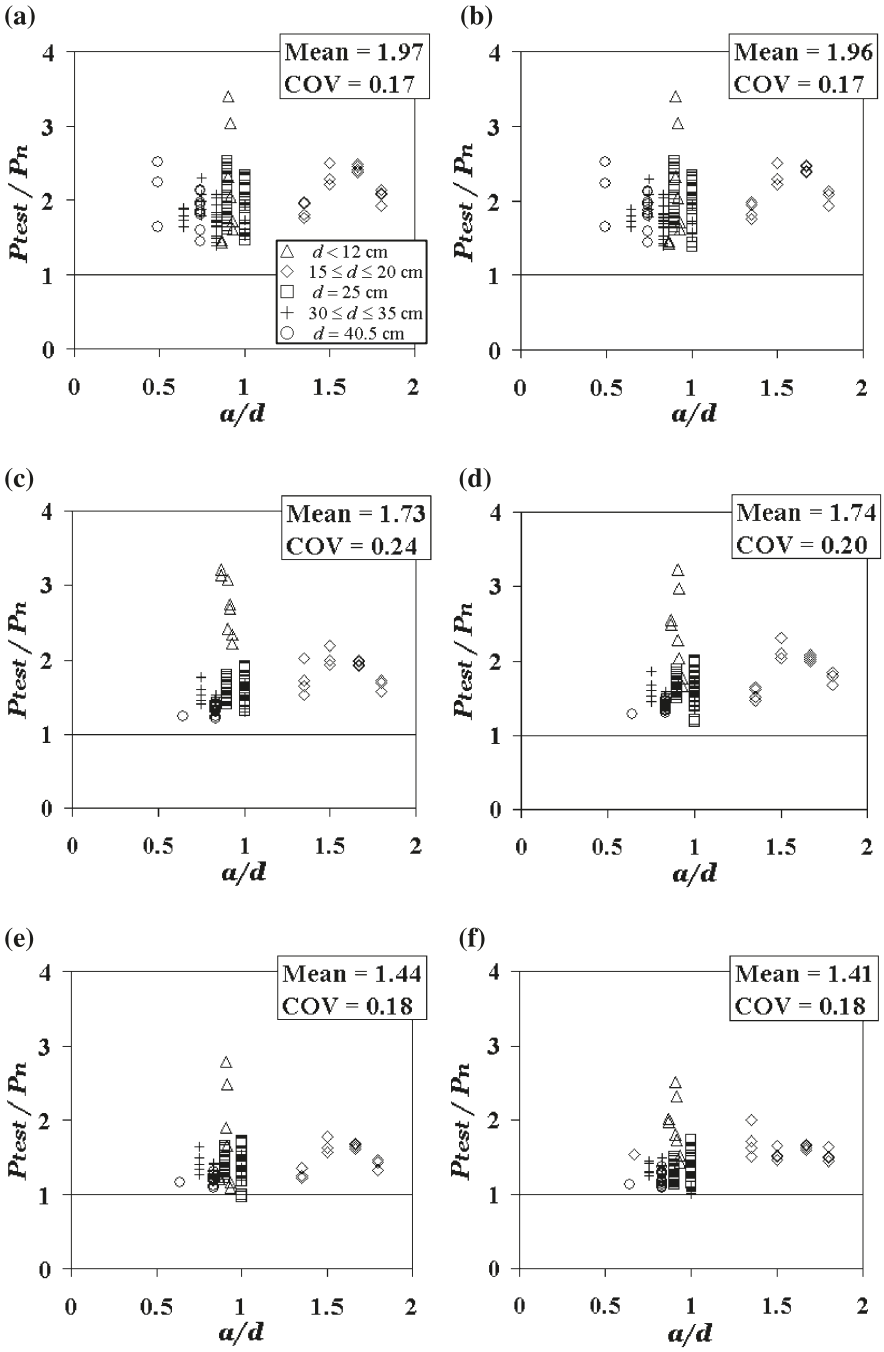

Committee 318 2005) minimum footing depth, and the specimens do not satisfy the code minimum depth of 305 and 300 mm in ACI and CSA, respectively. However, this test data was still used for the comparative evaluation, for the purpose of comparing the different design approaches.

Figure 2 presents the strength ratios (P_{test}/P_n) as a function of shear span-to-depth ratio for the six aforementioned methods: (*i*) special provisions for slabs and footings of ACI318–99; (*ii*) *CRSI design handbook* 2002, (*iii*) strut-and-tie model of ACI318–05, (*iv*) strut-and-tie model of CSA A23.3; (*v*) strut-and-tie model approach of Adebar and Zhou (1996), and (*vi*) proposed strut-and-tie model approach by the authors. Based on these comparisons, the following initial observations can be made. The special provisions in ACI318–99 and the design formula of the *CRSI design handbook* 2002 lead to the most conservative estimates of strength with very reasonable coefficients of variation for the range of tested pile caps. The strengths calculated by the strut-and-tie provisions in Appendix A of ACI318–05 and CSA A23.3 provide conservative estimates of capacities

Fig. 3. Ratio of measured to calculated strengths by shear failure mode with respect to shear span-to-depth ratio: (*a*) special provisions for slabs and footings of ACI318–99 (ACI Committee 318 1999); (*b*) *CRSI design handbook* 2002 (CRSI 2002); (*c*) strut-and-tie model of ACI318–05 (ACI Committee 318 2005); (*d*) strut-and-tie model of CSA A23.3 (CSA 2004); (*e*) strut-and-tie model approach of Adebar and Zhou (1996); (*f*) proposed strut-and-tie model approach. COV, coefficient of variation.

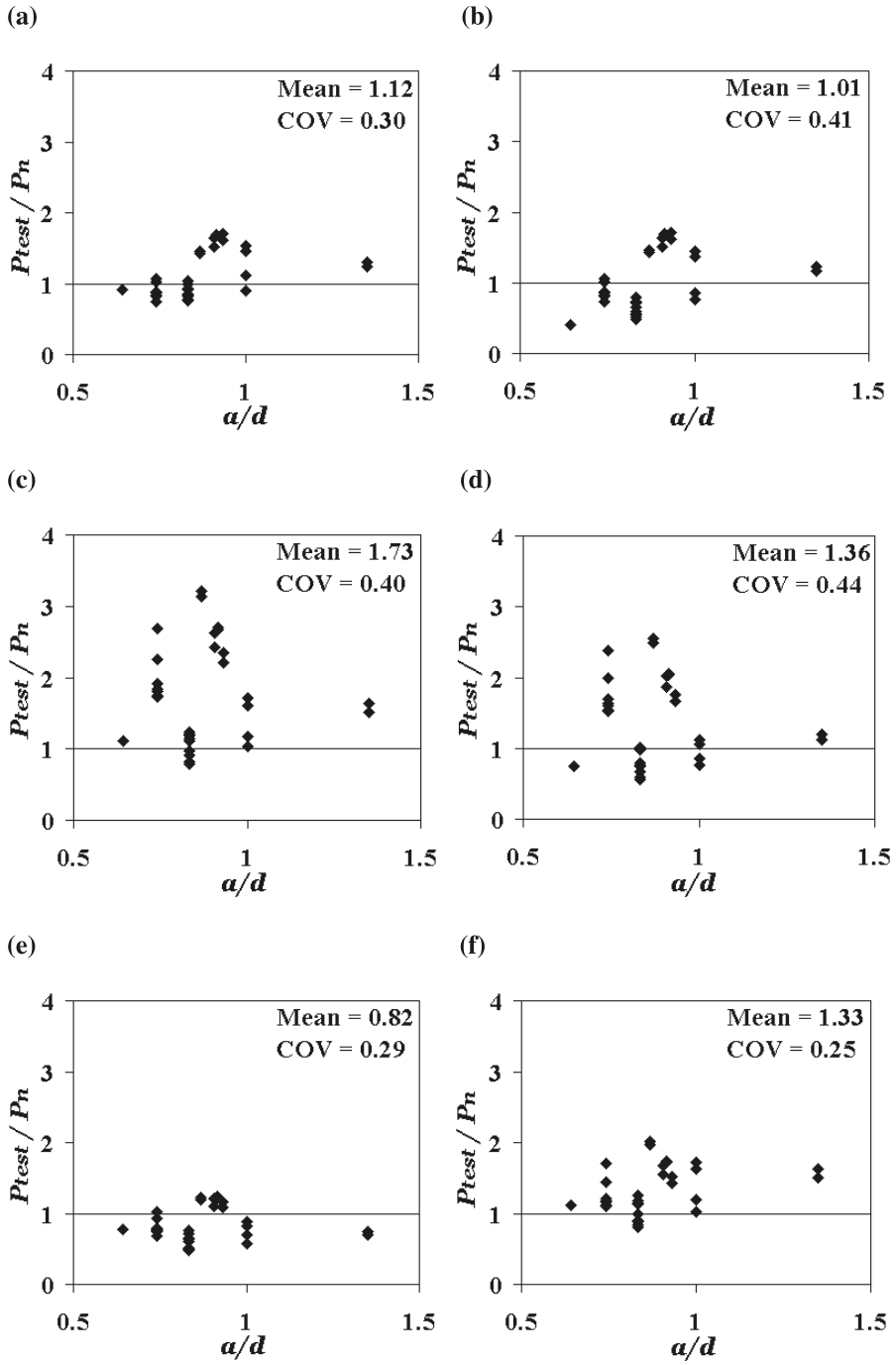

and somewhat larger scatter of strength ratios. The methods presented by Adebar and Zhou (1996) and the authors are less conservative, but still safe, with a scatter similar to that by the ACI and *CRSI design handbook* 2002 special provisions for footings and slabs.

The above observations were referred to as initial observations as a more complete examination of the behavior of the tested pile caps leads to a somewhat different assessment of the accuracy and safety of these methods. The source of the conservatism of the first four methods is that the calculated strength, P_n, was usually controlled by the calculated flexural capacity of the test structures. These calculated capacities have been observed to be unduly conservative due to inaccuracies in the estimated flexural lever arm and tensile contributions of the concrete that are ignored. Therefore, to evaluate the shear provisions and the strut and nodal zone stress limits of these methods, it is useful to examine the strength ratios for members that did not fail by reinforce-

Table 8. Test specimens reported to have failed by shear.

Author	Pile cap specimens
Clarke (1973)	A1, A2, A4, A5, A7, A8, A9, A10
Suzuki et al. (1998)	BP-25–1, BP-25–2, BP-30–30–1, BP-30–25–2
Suzuki et al. (1999)	BDA-40–25–70–1
Suzuki et al. (2000)	TDM3–1, TDM3–2
Suzuki and Otsuki (2002)	BPL-35–30–1, BPL-35–30–2, BPH-35–30–1, BPL-35–25–2, BPH-35–25–1, BPH-35–25–2, BPL-35–20–1, BPL-35–20–2, BPH-35–20–1, BPH-35–20–2
Sabnis and Gogate (1984)	SS1, SS2, SS3, SS4, SS5, SS6, SG2, SG3

ment yielding and in which the calculated strengths are not limited by the calculated flexural capacity or strength of the tension ties.

Figure 3 presents the strength ratios (P_{test}/P_n) as a function of shear span-to-depth ratio for the six aforementioned methods for only those 33 pile caps that were reported by the authors to have failed in shear and before reinforcement yielding and in which the nominal strength, P_n, is controlled by the calculated shear strength or strength of struts and nodes. As shown in Fig. 3, this leads to a very different impression of the accuracy and safety of these methods. The calculated shear capacities by ACI318–99 (Fig. 3*a*) and the *CRSI design handbook* 2002 (Fig. 3*b*) were unconservative in 17 and 19 of the 33 cases, respectively. The strut-and-tie provisions of ACI318–05 (Fig. 3*c*) and CSA A23.3 (Fig. 3*d*) were unconservative in 5 and 12 of the 33 cases, respectively. Thus, it can be concluded that whereas these four methods are conservative due to their underprediction of flexural and tie capacities, the shear, concrete strut, and nodal zone capacities predicted by these methods are unconservative.

Figure 3*e* examines the accuracy of the strut-and-tie model approach proposed by Adebar and Zhou (1996). The shear capacity predicted by this method is limited by the nodal zone bearing stresses given by eq. [2], and the flexural capacity can be described by the column load that would cause yielding of the steel tie of the strut-and-tie model. Adebar and Zhou (1996) assumed that the lower nodes of the strut-and-tie model were located at the center of the piles at the level of the longitudinal reinforcement, whereas the upper nodal zones were assumed to be at the top surface of the pile cap. As the inclination of the diagonal strut depends on the upper node location, the node location influences the strength prediction by eqs. [2] and [4]. This method does not overpredict any of the pile cap strengths and the predictions are reasonably conservative as the strength of most pile caps was limited by the conservative method for calculating the flexural capacity. However, the bearing capacity requirement provides unconservative estimations of the strengths for many specimens that were reported to have failed by shear, as shown in Fig. 3*e*. The shear span-to-depth ratios of most test specimens reviewed in this study is less than one, and the majority of the specimens may be more accurately described as combined bending and shear failure due to interpretation of failure modes. The nodal zone bearing stress limit calculated in eq. [2] results in similar maximum bearing strengths as calculated in the ACI code in which the stress limit is $\phi(0.85f'_c)\sqrt{A_2/A_1}$. Figure 3*e* illustrates that the bearing strength limit of eq. [2] is not a good indicator for pile cap strengths as has been reported by Cavers and Fenton (2004).

Figures 2*f* and 3*f* examine the accuracy of the procedure developed by the authors. The calculated capacities by the proposed method are both accurate and conservative with limited scatter or trends for pile caps with shear span-to-depth ratios ranging from 0.49 to 1.8 and a concrete strength less than 41 MPa. The proposed method also provides reasonably conservative strength predictions for all the specimens that were reported to have failed in shear. In an effort to accurately assess the mode of failure, the authors reviewed the strain distributions in the longitudinal reinforcement as well as the overall load–deflection curves in the 94 specimens tested by Suzuki et al. (1998, 1999, 2000; Suzuki and Otsuki 2002). The flexural yield was defined as the point in the load–deformation response where the deflection increased rapidly without significant load increase. As shown in Table 9, the mode of failure is estimated to have been successfully predicted in 72% of the cases by the proposed method. As the failure modes of many pile caps may be described more accurately as combined bending and shear failure even for the case of bending yield, the nominal strengths calculated from two or more different failure modes may not be as different as this comparison suggests.

Conclusions

In this paper, a three-dimensional strut-and-tie model approach has been presented for calculating the load-carrying capacity of pile caps. The failure strength predictions for 116 tested pile caps by this method are compared with those of six methods.

(1) The special provisions for slabs and footings of ACI318–99 (ACI Committee 318 1999) and the CRSI methods provided the most conservative strength predictions. This conservatism is due to the particularly low estimates of flexural capacity by these methods. If the shear provisions of these methods are used to predict the capacity of those members that are reported to have failed in shear, then these shear provisions are found to be quite unconservative; the capacity of more than one-half of the tested shear-critical pile caps are overpredicted.

(2) The strut-and-tie model approaches in Appendix A of ACI318–05 (ACI Committee 318 2005) and CSA A23.3 (CSA 2004) did not overpredict the measured strengths of any of the pile caps. However, the provisions of these methods for calculating the strength of struts and nodes by these methods were found to be somewhat unconservative for those members that did not fail by reinforcement yielding.

(3) The strut-and-tie approach by Adebar and Zhou (1996) did not overpredict the strength of any of the pile caps that failed by yielding of the longitudinal reinforcement

Table 9. Prediction of failure modes.

Specimen	Observed	Predicted
BP-20–1	B	S
BP-20–2	B	S
BPC-20–1	B	B
BPC-20–2	B	S
BP-25–1	S	S
BP-25–2	S	S
BPC-25–1	B	S
BPC-25–2	B	S
BP-20–30–1	B	B
BP-20–30–2	B	B
BPC-20–30–1	B	B
BPC-20–30–2	B	B
BP-30–30–1	S	B
BP-30–30–2	B	B
BPC-30–30–1	B	B
BPC-30–30–2	B	B
BP-30–25–1	B	B
BP-30–25–2	S	B
BPC-30–25–1	B	B
BPC-30–25–2	B	B
BDA-70–90–1	B	B
BDA-70–90–2	B	B
BDA-80–90–1	B	B
BDA-80–90–2	B	B
BDA-90–90–1	B	B
BDA-90–90–2	B	B
BDA-100–90–1	B	B
BDA-100–90–2	B	B
TDL1–1	B	B
TDL1–2	B	B
TDL2–1	B	B
TDL2–2	B	B
TDL3–1	B	B
TDL3–2	B	B
TDS1–1	B	B
TDS1–2	B	B
TDS2–1	B	B
TDS2–2	B	B
TDS3–1	B	S
TDS3–2	B	S
TDM1–1	B	B
TDM1–2	B	B
TDM2–1	B	B
TDM2–2	B	B
TDM3–1	S	S
TDM3–2	S	S
BDA-20–25–70–1	B	B
BDA-20–25–70–2	B	B
BDA-20–25–80–1	B	B
BDA-20–25–80–2	B	B
BDA-20–25–90–1	B	B
BDA-20–25–90–2	B	B
BDA-30–20–70–1	B	B
BDA-30–20–70–2	B	B
BDA-30–20–80–1	B	B
BDA-30–20–80–2	B	B
BDA-30–20–90–1	B	B

Table 9 (*concluded*).

Specimen	Observed	Predicted
BDA-30–20–90–2	B	B
BDA-30–25–70–1	B	B
BDA-30–25–70–2	B	B
BDA-30–25–80–1	B	B
BDA-30–25–80–2	B	B
BDA-30–25–90–1	B	B
BDA-30–25–90–2	B	B
BDA-30–30–70–1	B	B
BDA-30–30–70–2	B	B
BDA-30–30–80–1	B	B
BDA-30–30–80–2	B	B
BDA-30–30–90–1	B	B
BDA-30–30–90–2	B	B
BDA-40–25–70–1	S	S
BDA-40–25–70–2	B	S
BDA-40–25–80–1	B	S
BDA-40–25–80–2	B	S
BDA-40–25–90–1	B	S
BDA-40–25–90–2	B	S
BPL-35–30–1	S	S
BPL-35–30–2	S	S
BPB-35–30–1	B	S
BPB-35–30–2	B	S
BPH-35–30–1	S	B
BPH-35–30–2	B	B
BPL-35–25–1	B	B
BPL-35–25–2	S	B
BPB-35–25–1	B	S
BPB-35–25–2	B	S
BPH-35–25–1	S	B
BPH-35–25–2	S	B
BPL-35–20–1	S	S
BPL-35–20–2	S	S
BPB-35–20–1	B	S
BPB-35–20–2	B	S
BPH-35–20–1	S	B
BPH-35–20–2	S	B

and these strength predictions were reasonably accurate. However, this approach provided somewhat unconservative estimations of the shear strengths for many of the test specimens that were reported to have failed by shear.

(4) The calculated capacities by the proposed method were both accurate and conservative with little scatter or trends for tested pile caps with shear span-to-depth ratios ranging from 0.49 to 1.8 and a concrete strength less than 41 MPa. The success of the proposed method indicates that a strut-and-tie design philosophy is appropriate for the design of pile caps.

References

AASHTO. 1994. AASHTO LRFD bridge design specifications, American Association of State Highway Transportation Officials, Washington, D.C.

ACI Committee 318. 1999. Building code requirements for reinforced concrete (ACI318–99) and commentary (ACI318R–99). American Concrete Institute, Farmington Hills, Mich.

ACI Committee 318. 2002. Building code requirements for reinforced concrete (ACI318–02) and commentary (ACI318R–02). American Concrete Institute, Farmington Hills, Mich.

ACI Committee 318. 2005. Building code requirements for reinforced concrete (ACI318–05) and commentary (ACI318R–05). American Concrete Institute, Farmington Hills, Mich.

Adebar, P., and Zhou, Z. 1993. Bearing strength of compressive struts confined by plain concrete. ACI Structural Journal, **90**(5): 534–541.

Adebar, P., and Zhou, Z. 1996. Design of deep pile caps by strut-and-tie models. ACI Structural Journal, **93**(4): 437–448.

Adebar, P., Kuchma, D., and Collins, M.P. 1990. Strut-and-tie models for the design of pile caps: An experimental study. ACI Structural Journal, **87**(1): 81–92.

Blévot, J., and Frémy, R. 1967. Semelles sur pieux. Annales de l'Institut Technique du Batiment et des Travaux Publics, **20**(230): 223–295. [In French.]

Bloodworth, A.G., Jackson, P.A., and Lee, M.M.K. 2003. Strength of reinforced concrete pile caps. Proceedings of the Institution of Civil Engineers, Structures & Buildings, **156**(4): 347–358. doi:10.1680/stbu.156.4.347.37843.

Cavers, W., and Fenton, G.A. 2004. An evaluation of pile cap design methods in accordance with the Canadian design standard. Canadian Journal of Civil Engineering, **31**(1): 109–119. doi:10.1139/l03-075.

Clarke, J.L. 1973. Behavior and design of pile caps with four piles. Cement and Concrete Association, London. Report No. 42.489.

CSA. 1984. Design of concrete structures for buildings. Standard A23.3–M84, Canadian Standards Association, Mississauga, Ont.

CSA. 2004. Design of concrete structures for buildings. Standard A23.3–M04, Canadian Standards Association, Mississauga, Ont.

CRSI. 2002. CRSI design handbook. Concrete Reinforcing Steel Institute, Schaumburg, Ill.

Foster, S.J., and Gilbert, R.I. 1996. The design of nonflexural members with normal and high-strength concretes. ACI Structural Journal, **93**(1): 3–10.

Hsu, T.T.C., and Zhang, L.X.B. 1997. Nonlinear analysis of membrane elements by fixed-angle softened-truss model. ACI Structural Journal, **94**(5): 483–492.

Kim, H.J., Mission, J.L.C., and Park, I.S. 2007. Analysis of static axial load capacity of single piles and large diameter shafts using nonlinear load transfer curves. KSCE Journal of Civil Engineering, **11**(6): 285–292. doi:10.1007/BF02885899.

Martinez, S., Nilson, A.H., and Slate, F.O. 1982. Spirally-reinforced high-strength concrete columns. Department of Structural Engineering, Cornell University, Ithaca, N.Y. Research report No. 82–10.

Park, J.W., and Kuchma, D. 2007. Strut-and-tie model analysis for strength prediction of deep beams. ACI Structural Journal, **104**(6): 657–666.

Paulay, T., and Priestley, M.J.N. 1992. Seismic design of reinforced concrete and masonry buildings. John Wiley and Sons, New York.

Sabnis, G.M., and Gogate, A.B. 1984. Investigation of thick slab (pile cap) behavior. ACI Journal, **81**(1): 35–39.

Schlaich, J., Schäfer, K., and Jennewein, M. 1987. Toward a consistent design of reinforced structural concrete. Journal of Prestressed Concrete Institute, **32**(3): 74–150.

Suzuki, K., and Otsuki, K. 2002. Experimental study on corner shear failure of pile caps. Transactions of the Japan Concrete Institute, **23**: 303–310.

Suzuki, K., Otsuki, K., and Tsubata, T. 1998. Influence of bar arrangement on ultimate strength of four-pile caps. Transactions of the Japan Concrete Institute, **20**: 195–202.

Suzuki, K., Otsuki, K., and Tsubata, T. 1999. Experimental study on four-pile caps with taper. Transactions of the Japan Concrete Institute, **21**: 327–334.

Suzuki, K., Otsuki, K., and Tsuchiya, T. 2000. Influence of edge distance on failure mechanism of pile caps. Transactions of the Japan Concrete Institute, **22**: 361–368.

Vecchio, F.J., and Collins, M.P. 1982. Response of reinforced concrete to in-plane shear and normal stresses. University of Toronto, Toronto, Ont. Report No. 82–03.

Vecchio, F.J., and Collins, M.P. 1986. Modified compression field theory for reinforced concrete elements subjected to shear. ACI Journal, **83**(2): 219–231.

Vecchio, F.J., and Collins, M.P. 1993. Compression response of cracked reinforced concrete. Journal of Structural Engineering, **119**(12): 3590–3610. doi:10.1061/(ASCE)0733-9445(1993)119:12(3590).

List of symbols

a	distance from pile centerline to column centerline measured parallel to pile cap side
A_1	loading area
A_2	supporting surface area
A_{ct},	effective areas of concrete tie
A_d	effective areas of diagonal strut
A_g	gross area of the column section
A_s	cross-sectional area of main reinforcement
A_{st}	area of tie reinforcement
b_s	width of compression strut
c	column size
d	effective depth
d_p	pile diameter
E_c	modulus of elasticity of concrete
E_s	modulus of elasticity of steel reinforcement
f_b	maximum bearing strength
f'_c	compressive strength of concrete cylinder
f_{cr}	concrete tensile strength
f_{ct}	tensile stress of concrete tie
f_y	yield strength of reinforcement
F_{ct}	nominal strength of concrete tie
F_d, F_x, F_y	the forces of diagonal, x-, and y-directional members
F_{st}	capacity of steel tie reinforcement
h	overall height
h_c	overall height of the column section
h_s	height of the strut
k	fluxural compression capacity factor
l_e	pile spacing
n	ratio of steel to concrete elastic moduli
N	compression force acting on the column
P	column load
P_n	nominal strength
P_{test}	measured capacity of test structure
V_c	contribution of concrete to shear capacity
w	distance between column face and center line of pile
w_c	effective width of horizontal strut
α	strut confinement factor
β	strut geometry factor
ε_0	strain at peak stress of standard cylinder
ε_d	compressive strain of diagonal strut
ε_h, ε_v	strain of horizontal direction and vertical direction

ε_r tensile strain of the direction perpendicular to diagonal strut
ε_s, ε_{st} tensile strain of steel tie
θ_x, θ_y, θ_z inclination angle between diagonal strut and x-, y-, and z-axis
ξ concrete-softening coefficient
ρ ratio of longitudinal reinforcement
σ_d compressive stress of concrete strut
ϕ strength reduction factor